www.czasopisma.pan.pl PAN POLSKA AKADEMIA NAUK www.journals.pan.pl

Arch. Metall. Mater. **68** (2023), 2, 607-616

DOI: https://doi.org/10.24425/amm.2023.142441

TEMEL SAVAŞKAN[1], HASAN ONUR TAN[2*]

EFFECT OF OPERATING CONDITIONS ON THE TRIBOLOGICAL BEHAVIOR OF Zn-30Al-3Cu BEARING ALLOY

To determine the relationships between operating conditions and tribological properties of Zn-30Al-3Cu alloy, its wear characteristics were investigated at wide ranges of oil flow rate, pressure and sliding velocity using a block-on-disk type test apparatus. The results are compared to those of SAE 660 leaded bearing bronze. Wear loss of these materials increased with sliding distance, pressure and sliding velocity, but decreased slightly with oil flow rate. The relationships between operating conditions and lubricated wear properties of Zn-30Al-3Cu alloy were determined by nonlinear regression analysis of the experimental data. Lubricated wear behavior of the zinc-based alloy was discussed in terms its microstructure and mechanical properties, and test conditions.

Keywords: Zn-30Al-3Cu alloy; Sliding friction; Lubricated wear; Running condition-wear property relationship

1. Introduction

Zinc-based commercial alloys began to appear in the market in the late 1920s [1-3]. During the Second World War due to the difficulties encountered in the supply of conventional bearing materials, efforts were made to develop new zinc-based bearing alloys [4-6]. Extensive and intensive research on these alloys resulted in the development of several engineering materials such as ZA-8, ZA-12, ZA-27, ALZEN 305 and ALZEN 501 [7-11]. These studies also showed that the zinc-based alloys have superior properties compared to traditional bearing alloys including white metal (Babbit), bronze, brass and cast iron [4-6,9,12-14]. These advantages can be stated as easy and economical production, good fluidity and castability, high specific strength, high wear resistance, good tribological behavior even in the case of insufficient lubrication and high damping capacity [6,7,15-17]. The commercial alloy designated as ALZEN 305 (Zn-30Al-5Cu) was the first zinc-based alloy developed for bearing applications. Research studies have led to the development of several Zn-30Al and Zn-40Al based alloys with copper and/or silicon [12,14,16,18]. Further studies showed that Zn-30Al-3Cu alloy has a perfect combination of strength, ductility, and wear resistance [18]. This means that it has the highest quality index value and wear resistance among the Zn-30Al-based ternary alloys [18]. Since copper is an expensive metal, the lower copper content of it provides economic advantages over the commercial ALZEN 305 alloy. Dry wear characteristics of this alloy have been studied at different pressures and sliding velocities [18]. However, the effects of operating parameters including contact pressure, sliding velocity and oil flow rate (OFR) on the lubricated wear characteristics of this alloy have not been investigated in a systemic manner. Moreover, the relationships between test parameters and lubricated wear behavior of this alloy have not been determined. Therefore, the aim of this study is to determine the relationships between the operating conditions (contact pressure, sliding velocity and oil flow rate) and tribological properties (friction coefficient, temperature, and wear loss) of Zn-30Al-3Cu alloy. This study can be considered as the continuation of the work reported in [18].

2. Materials and methods

Zn-30Al-3Cu alloy was produced by permanent mold casting as described in [18]. SAE 660 bearing bronze was also used in this work for comparison purposes. The zinc-based alloy and the bronze were analyzed by atomic absorption spectroscopy. Samples for metallography were prepared by standard procedures including molding, grinding, polishing, and etching. Zn-30Al-3Cu alloy was etched with % 20 Nital (% 20 nitric acid + % 80 ethanol). The microstructure of the zinc-based alloy was studied using a JEOL 6400 model scanning electron microscope (SEM) at an accelerating voltage of 15 kV. The phases in the

[1] HALIÇ UNIVERSITY, DEPARTMENT OF MECHANICAL ENGINEERING, 34060 EYÜPSULTAN, ISTANBUL, TURKEY
[2] GIRESUN UNIVERSITY, DEPARTMENT OF MECHANICAL ENGINEERING, 28200, GIRESUN, TURKEY
* Corresponding author: hasan.tan@giresun.edu.tr

microstructure were identified by metallographic examinations and energy dispersive X-ray spectroscopy (EDS) analysis. X-ray diffraction studies were also performed to verify the phases of the zinc-based alloy using CuK_{α} radiation the wavelength of which is 1.542 Å.

The hardness of the experimental materials was measured with a Rockwell hardness tester using the F scale and converted into Brinell hardness number. Tensile and compression tests were carried out on the specimens with the dimensions (diameter × length) of 10 mm × 50 mm and 10 mm × 10 mm at a strain rate of 4×10^{-3} s^{-1} according to TS 138 EN 10002-1 (ASTM E-8) and TS EN 206 (ASTM E-9) standards, respectively. The impact energy of both materials was measured by the Charpy method using the specimens with dimensions of 10 mm × 10 mm × 55 mm. as described in the literature [18]. The values of the mechanical properties were determined by taking the average of three measurements.

Lubricated wear properties of the zinc-based alloy and the bronze were studied with a block-on-disk type tester (Fig. 1). This wear tester simulates the contact between the shaft and the journal bearing to a certain extent. The disk was made from SAE 1045 steel (Fe-0.46%C-0.6%Mn-0.035%P-0.03%S) with a diameter of 200 mm. It was subjected to hardening and tempering treatment to obtain a hardness of 50 HRC. Wear specimens (block) with the size of 10 × 15 × 26.6 mm were prepared from the materials by milling and turning operations. The wear specimens and the disk were ground and polished to keep their average surface roughness below 1 µm. Surface roughness of the wear samples was measured by a contact type measuring device (MAHR MarSurf M 300) before and after each test. SAE 20W/50 engine oil was used as lubricant for the wear tests.

Two types of wear tests were carried out in this work. These were long and short distance tests. Long distance wear tests were conducted at a constant pressure (6 MPa), sliding velocity (2 ms^{-1}) and OFR (1 cm^3 h^{-1}) for a sliding distance (SD) of 108 km. The short distance wear tests were performed at eight different contact pressures (1-8 MPa), six different sliding velocities (0.5-3 ms^{-1}) and six different oil flow rates (OFRs) (0.5-3 cm^3 h^{-1}) for a SD of 20 km. The long-distance tests were applied to evaluate the general wear behavior of the zinc-based alloy and the bronze under moderate test conditions. However, the short distance tests were conducted to determine the relationships between the test parameters and the lubricated wear properties of these materials. The friction force was measured by a load cell and the friction coefficient (FC) of the zinc-based alloy and the bronze were determined by the ratio between friction and normal forces. The temperature of the wear specimens was measured by a T-type thermocouple (Cu-CuNi). The wear specimens were cleaned in an ultrasonic cleaner using trichloroethylene (C_2HCl_3) and ethanol-acetone mixture and then weighted to determine the mass loss using an analytical balance with a precision of 0.01 mg, before and after the tests. The contact surface of the disk

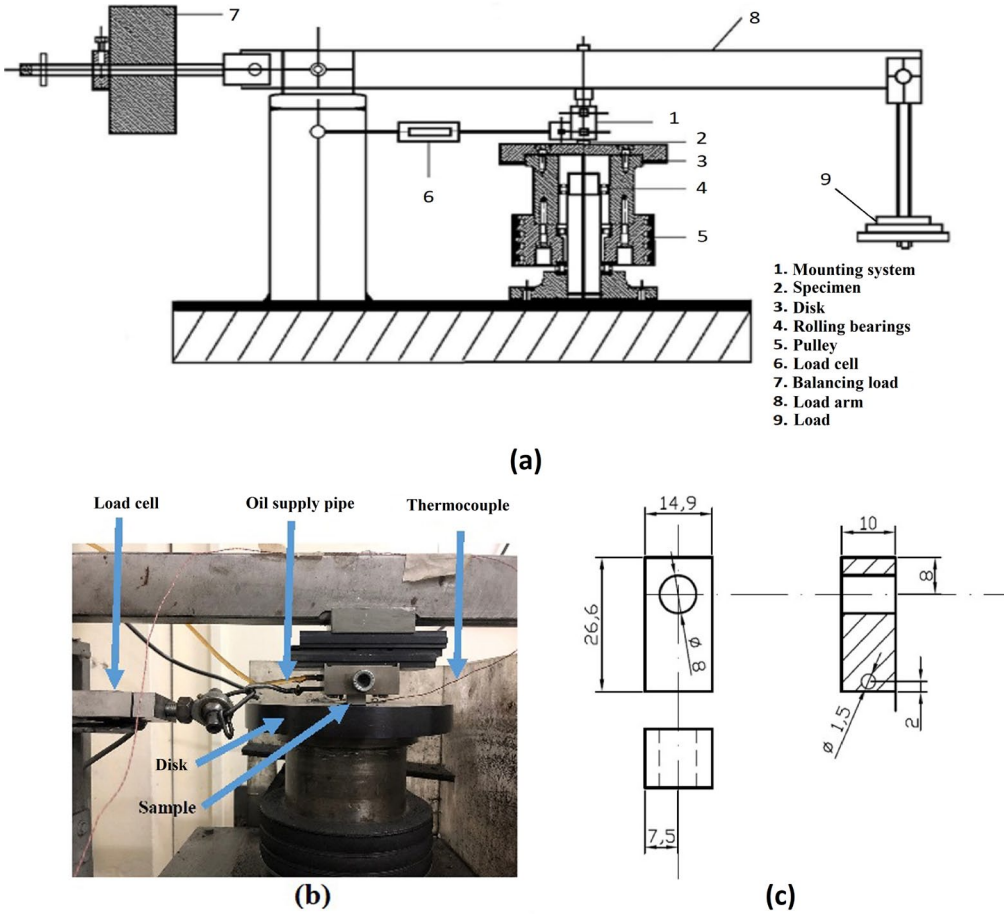

Fig. 1. (a) Schematic illustration and (b) close up view of the wear test machine, and (c) technical drawing of the wear test sample

was also cleaned with appropriate solvents before and after the tests. Some of the wear tests were repeated twice to obtain reliable results. Wear loss values were determined by calculating the mass loss/density ratios for the alloy and the bronze. Worn surfaces of the samples were studied using secondary electron (SE) imaging mode of SEM and EDS technique.

3. Results

Chemical compositions of the zinc-based alloy and the bronze are given in TABLE 1. The metallographic structure of Zn-30Al-3Cu alloy consisted of β dendrites, eutectoid mixture of α + η phases and intermetallic ε ($CuZn_4$) phases as shown in Fig. 2(a). The X-ray diffraction pattern obtained from this alloy confirmed the presence of the phases (α, β, η and ε) in its microstructure, Fig. 2(b). The microstructure of SAE 660 bearing bronze is composed of α dendrites, eutectoid mixture of α + δ phases and a lead phase, Fig. 3.

Relevant mechanical properties of the experimental materials are given in TABLE 2. This table shows that the zinc-based alloy has higher hardness and tensile strength but lower compressive strength, impact energy and elongation to fracture than the bronze.

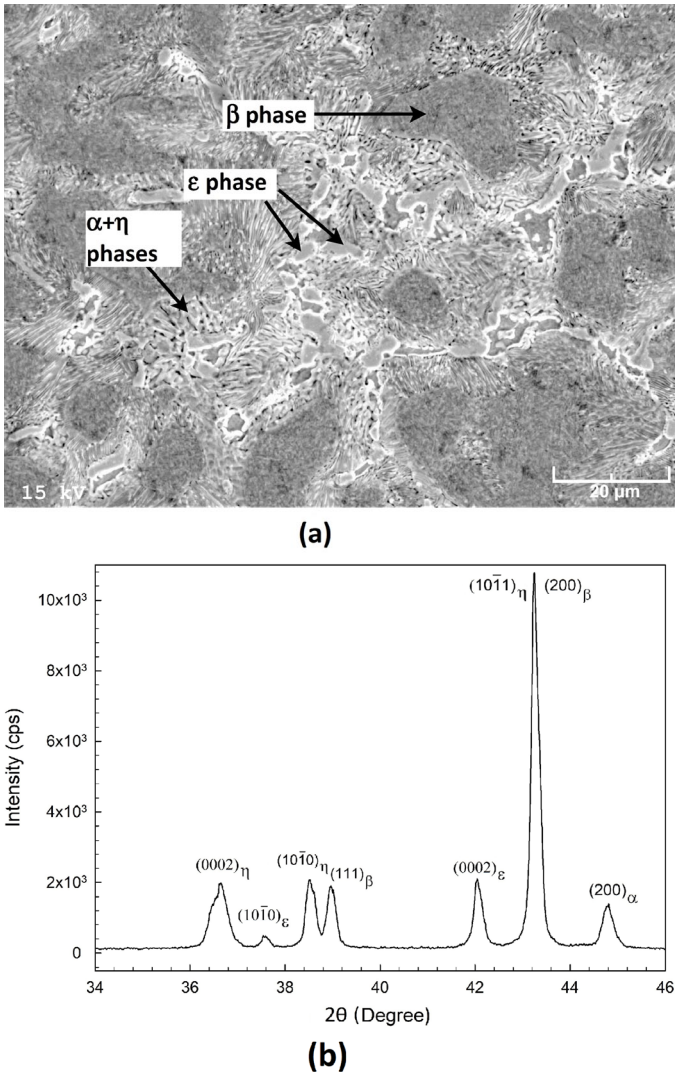

Fig. 2. (a) Metallographic structure and (b) X-ray diffraction pattern of Zn-30Al-3Cu alloy

TABLE 1

Chemical compositions of the alloy and the bronze

Material	Chemical composition (wt. %)				
	Zn	Al	Cu	Sn	Pb
Zn-30Al-3Cu alloy	67.1	29.8	3.1	—	—
SAE 660 bronze	2.6	—	83.9	7.1	6.4

Some wear tests were repeated twice and the differences between two readings were observed to be less than 2% of the mean value of the test parameters. This means that the measurement error or range of scatter had no noticeable effect on the shape and position of the friction coefficient, temperature and wear curves of the experimental materials.

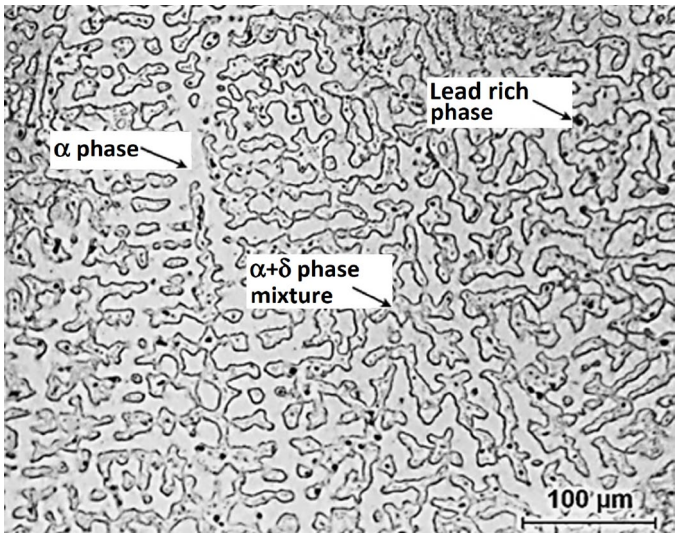

Fig. 3. Metallographic structure of SAE 660 leaded bronze

The plots showing the changes in FC, temperature, and wear loss of the test materials with SD are given in Fig. 4(a)-(c). The temperature in this study corresponds to the temperature of

TABLE 2

Mechanical properties of the experimental materials

Material	Hardness (BHN)	Ultimate tensile strength (MPa)	Compressive strength (MPa)	Impact energy (J)	Elongation to fracture (%)
Zn-30Al-3Cu alloy	104±4	350±6	870±10	3.5±1	10.3±0.8
SAE 660 bronze	87±3	280±5	1075±12	12.9±1.5	12±1

the specimens measured at the end of the wear tests. The curves of this figure show that the friction coefficient of both materials decreases at the early stage of the test and becomes constant after a SD of about 20 km. Their temperatures increased sharply with sliding velocity at the start of the test and reached steady states after a SD of about 20 km. However, the measured wear loss values increased with increasing SD.

The curves of FC, temperature, and wear loss of the experimental materials versus pressure are given in Fig. 5. These curves show that the FC of these materials decreases, but their temperature and wear loss rise with increasing pressure.

Fig. 6 shows the changes in FC, temperature, and wear loss of both materials with sliding velocity. All these parameters increased with increasing sliding velocity. The increasing trend is more evident above a sliding speed of 2 ms^{-1}.

The changes in FC, temperature, and wear loss of the test materials with OFR are presented in Fig. 7. The FC, temperature and wear loss of the experimental materials decreased as the

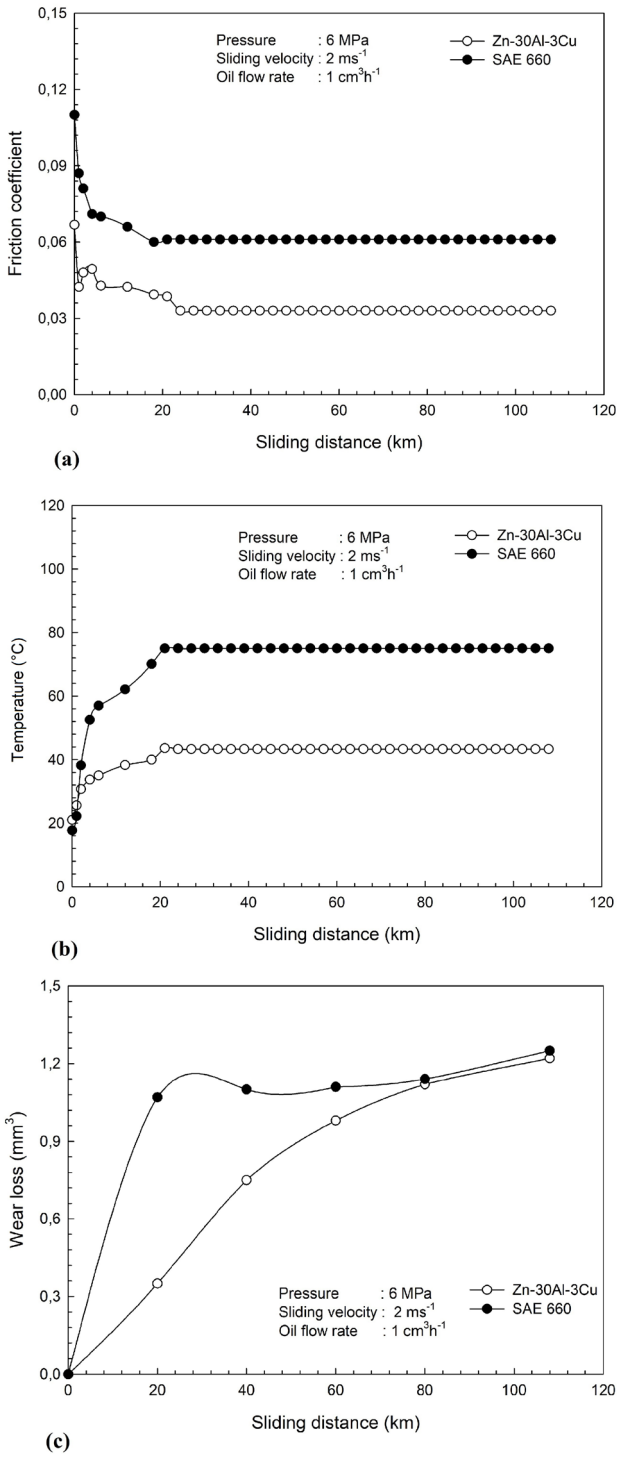

Fig. 4. Plots of (a) FC, (b) temperature and (c) wear loss versus SD for the alloy and the bronze tested at the given pressure, sliding velocity and OFR for a SD of 108 km

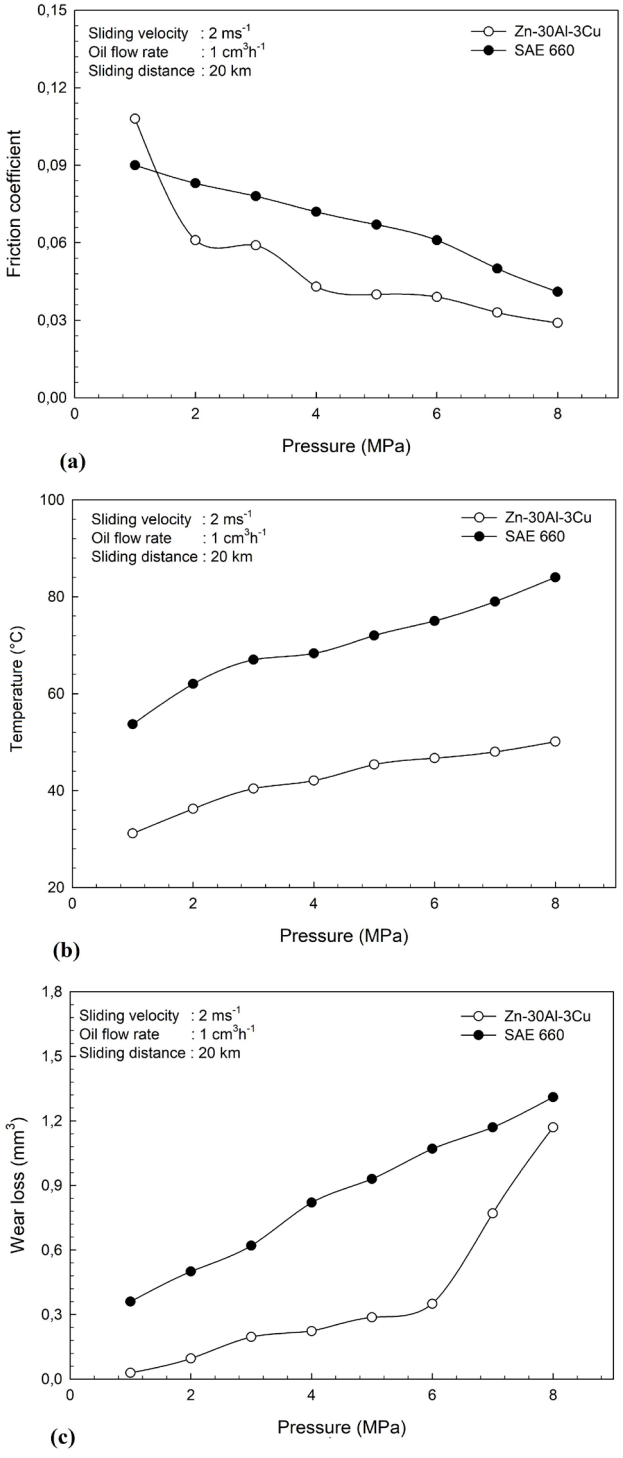

Fig. 5. Plots of (a) FC, (b) temperature and (c) wear loss versus pressure for the materials tested at the given sliding velocity and OFR for a SD of 20 km

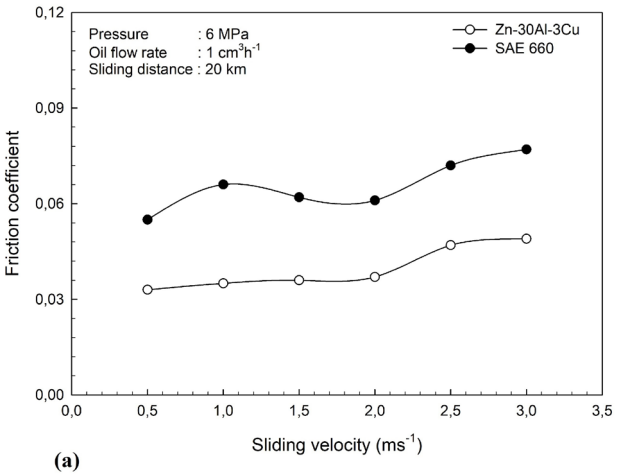

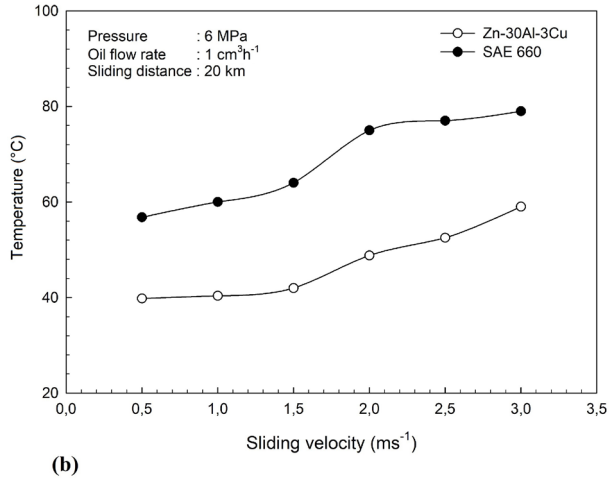

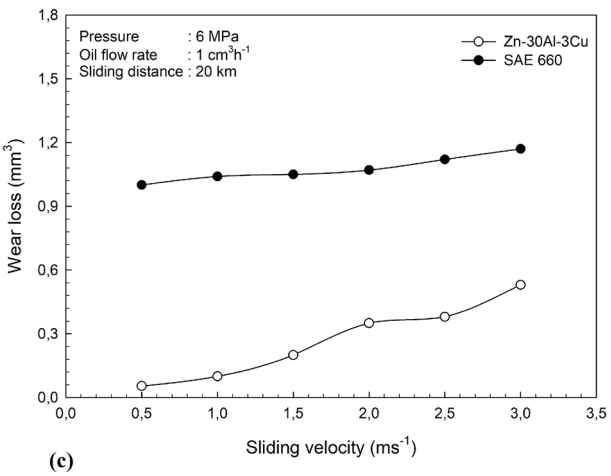

Fig. 6. Plots of (a) FC, (b) temperature and (c) wear loss versus sliding velocity for the experimental materials tested at the given pressure and OFR for a SD of 20 km

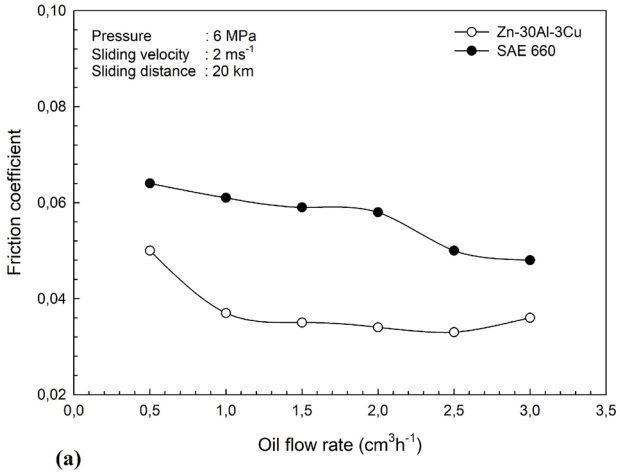

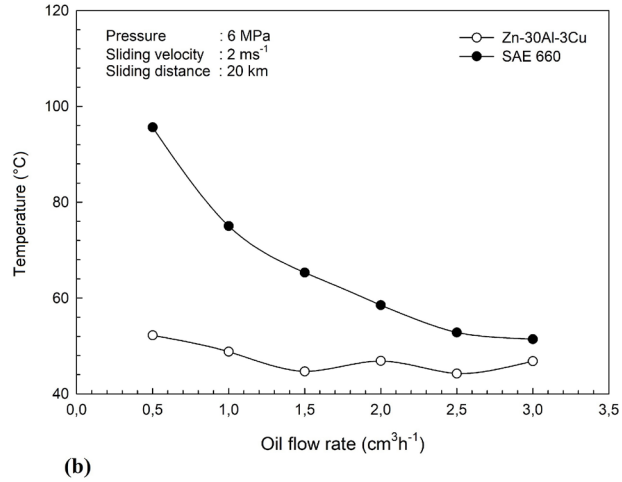

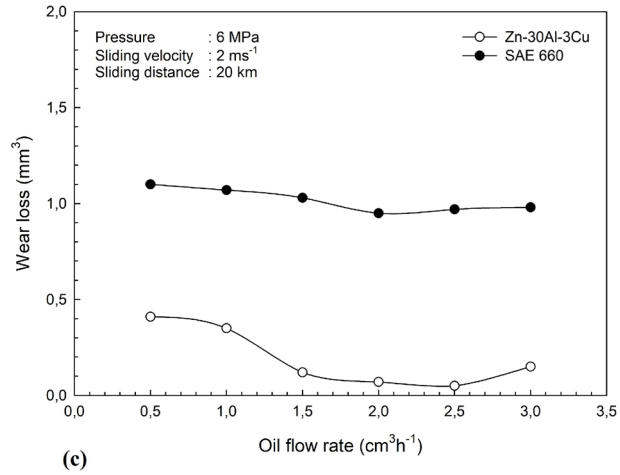

Fig. 7. Plots of (a) FC, (b) temperature and (c) wear loss versus OFR for the experimental materials tested at the given pressure and sliding speed for a SD of 20 km

OFR increased. However, above an OFR of 2.5 $cm^3\ h^{-1}$, these properties of the alloy showed a slight increase. All these plots show that under all the operating conditions, Zn-30Al-3Cu alloy exhibits lower FC, temperature, and wear loss than the bronze.

Three-dimensional (3D) plots showing the effect of both pressure and sliding velocity on the FC, temperature, and wear loss of Zn-30Al-3Cu alloy are given in Fig. 8(a)-(c). The FC of the alloy increased with increasing velocity but decreased as the pressure increased. However, its temperature and wear loss increased with these parameters.

Worn surfaces of the specimens of the zinc-based alloy were characterized mainly by smearing of the adhered material, Figs. 9-11. These micrographs show that the area of the smeared region on the worn surface of the alloy samples increased with increasing pressure and sliding velocity. The worn surfaces of the bronze samples revealed both smeared material and scratches,

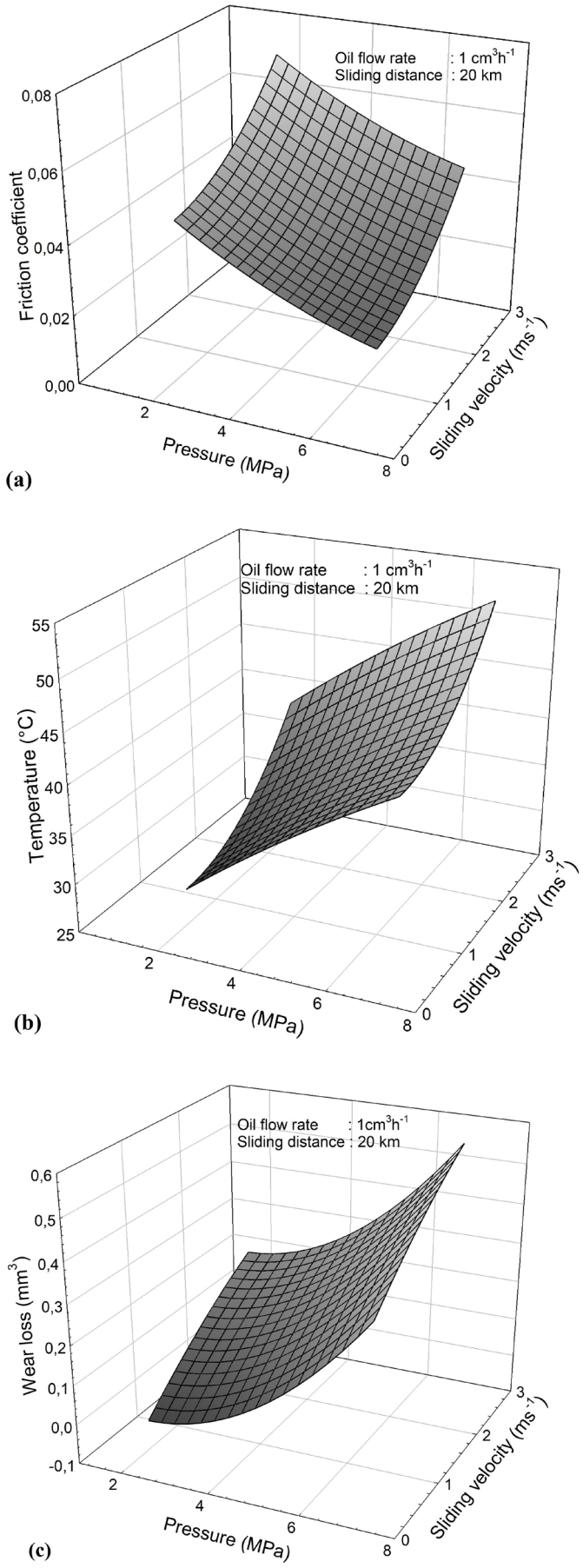

Fig. 8. 3D plots showing the effect of pressure and sliding velocity on (a) FC, (b) temperature and (c) wear loss of Zn-30Al-3Cu alloy tested at an OFR of 1cm^3 h^{-1} for a SD of 20 km

Fig. 12. It was observed that the area of the smeared region and the number of scratches increased as the pressure and sliding velocity was raised. However, OFR showed no regular effect on the worn surface characteristics of both the alloy and the bronze. No microstructural alterations were noticed under the worn surface of the alloy and the bronze, as shown in Fig. 13(a) and (b).

4. Discussion

The structure of Zn-30Al-3Cu alloy is composed of the zinc-rich η and β phases, eutectoid mixture of (α + η) and ε ($CuZn_4$) particles, Fig. 2a. Occurrence of this microstructure was attributed to the phase changes that occur during solidification of the alloy and solid solubility of copper in zinc and aluminum [18-22].

The friction coefficient of both materials subjected to wear test at constant pressure (6 MPa), sliding velocity (2 ms^{-1}) and OFR of 1 cm^3 h^{-1} for a SD of 108 km, decreased rapidly at the beginning of the test, Fig. 4(a). However, their temperatures increased rapidly and reached constant levels at a SD of about 20 km, Fig. 4(b). The wear loss values also showed a rapid increase at the start of the test, but the rate of increase decreased as the SD increased, Fig. 4(c). The rapid decrement in the friction coefficient at the beginning of the wear tests is due to the transition from dry to lubricated friction, but the rapid increase in temperature and wear volume values can be attributed to the sample and disk contact that occurs due to insufficient oil film thickness (OFT) [22-24]. The OFT increases with increasing SD, and when it becomes sufficient to separate the rubbing surfaces both the FC and the temperature reach steady states.

The friction coefficients of both materials subjected to wear tests at constant sliding speed (2 ms^{-1}) and OFR (1 cm^3 h^{-1}) decreased, but their temperature and wear loss increased with rising pressure, Fig. 5(a)-(c). This observation may be related to the lubrication regime. According to Stribeck curve, the FC of the lubricated systems decreases with increasing contact pressure only in the hydrodynamic or full film lubrication regime [17,23,24]. In addition, as the pressure increases the OFT decreases. This results in a decrement in the FC by reducing the friction between the oil molecules. The increase in their temperature and wear loss may be attributed to the rise in the contact area, friction force and frictional heat with increasing pressure especially in the running-in period.

FC, temperature, and wear loss of the materials tested at constant pressure (6 MPa) and OFR (1 cm^3 h^{-1}) increased with rising sliding velocity, and the increase became more evident above a sliding velocity of 2 ms^{-1}, Fig. 6(a)-(c). This can be related to the centrifugal force acting on the lubricating oil. As the sliding velocity rises, the centrifugal force acting on the oil increases. Increased centrifugal force causes more oil to be scattered away or removed from the disk surface. This gives rise to a decrement in the amount of oil and the OFT between the disk and the sample surfaces. In this case, the cooling effect of the lubricating oil decreases. In addition, as the sliding velocity increases, it becomes difficult to remove the frictional heat

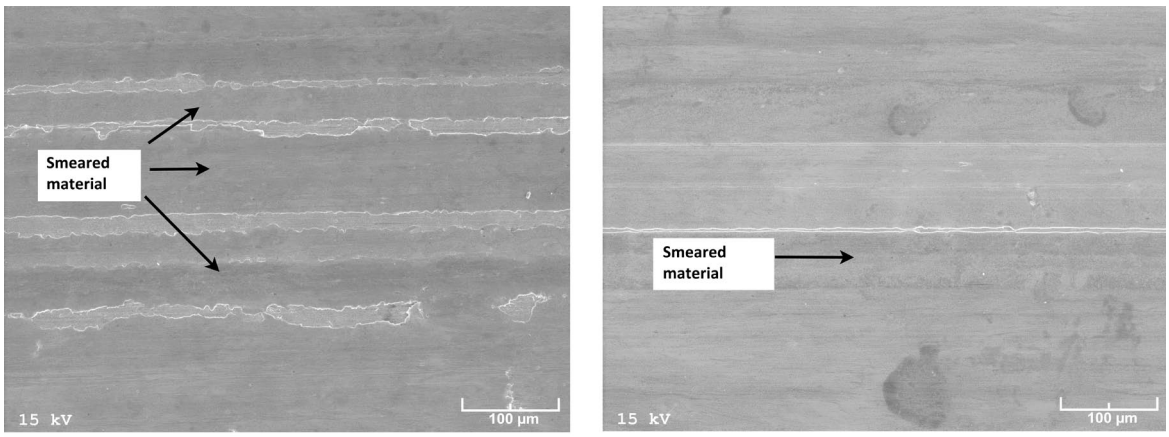

Fig. 9. SEM micrographs showing the worn surfaces of the alloy tested at constant OFR (1 $cm^3\ h^{-1}$) and sliding velocity (2 ms^{-1}), but different pressures of (a) 1 MPa and (b) 8 MPa for a SD of 20 km

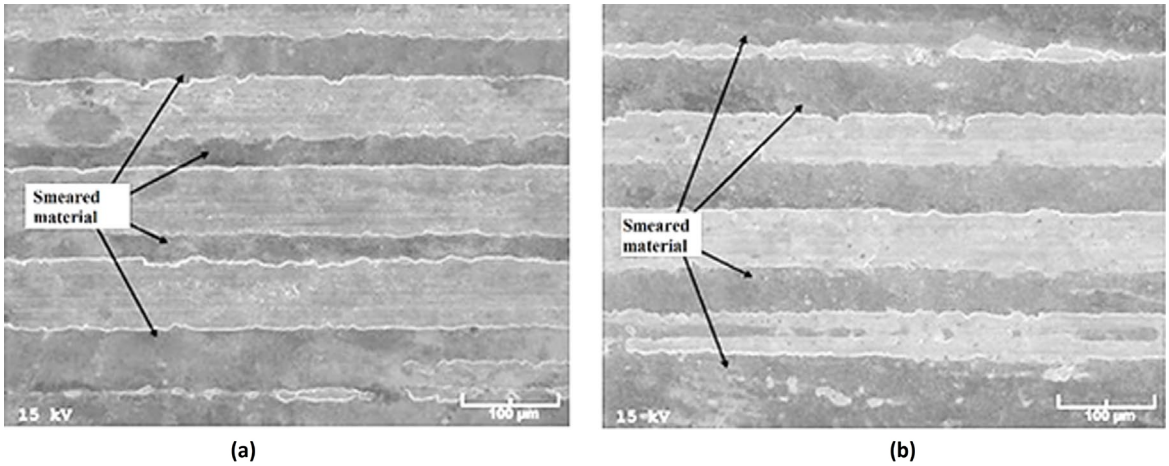

Fig. 10. Worn surfaces of the alloy tested at constant OFR (1 $cm^3\ h^{-1}$) and pressure (6 MPa), but different sliding velocities of (a) 0.5 ms^{-1} and (b) 2.5 ms^{-1} for a SD of 20 km

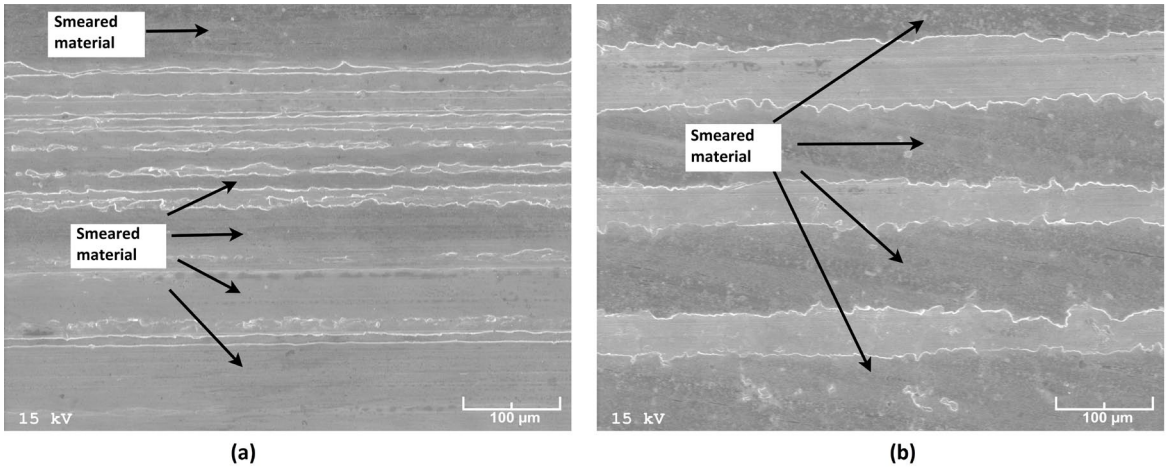

Fig. 11. Worn surfaces of the alloy tested at constant pressure (6 MPa) and sliding velocity (2 ms^{-1}), but different OFRs of (a) 0.5 $cm^3\ h^{-1}$ and (b) 3 $cm^3\ h^{-1}$ for a SD of 20 km

from the surfaces due to lack of time. For these reasons, as the sliding velocity increases, the temperatures of the alloy and the bronze increase. As the temperature increases, the viscosity of the lubricating oil decreases, and this causes a decrement in the friction between the oil molecules. The increase in the wear loss can be related to metal-to-metal contact that occurs mainly during the running-in stage. Although the increase in sliding velocity shortens the test period, the increase in the amount of oil scattered

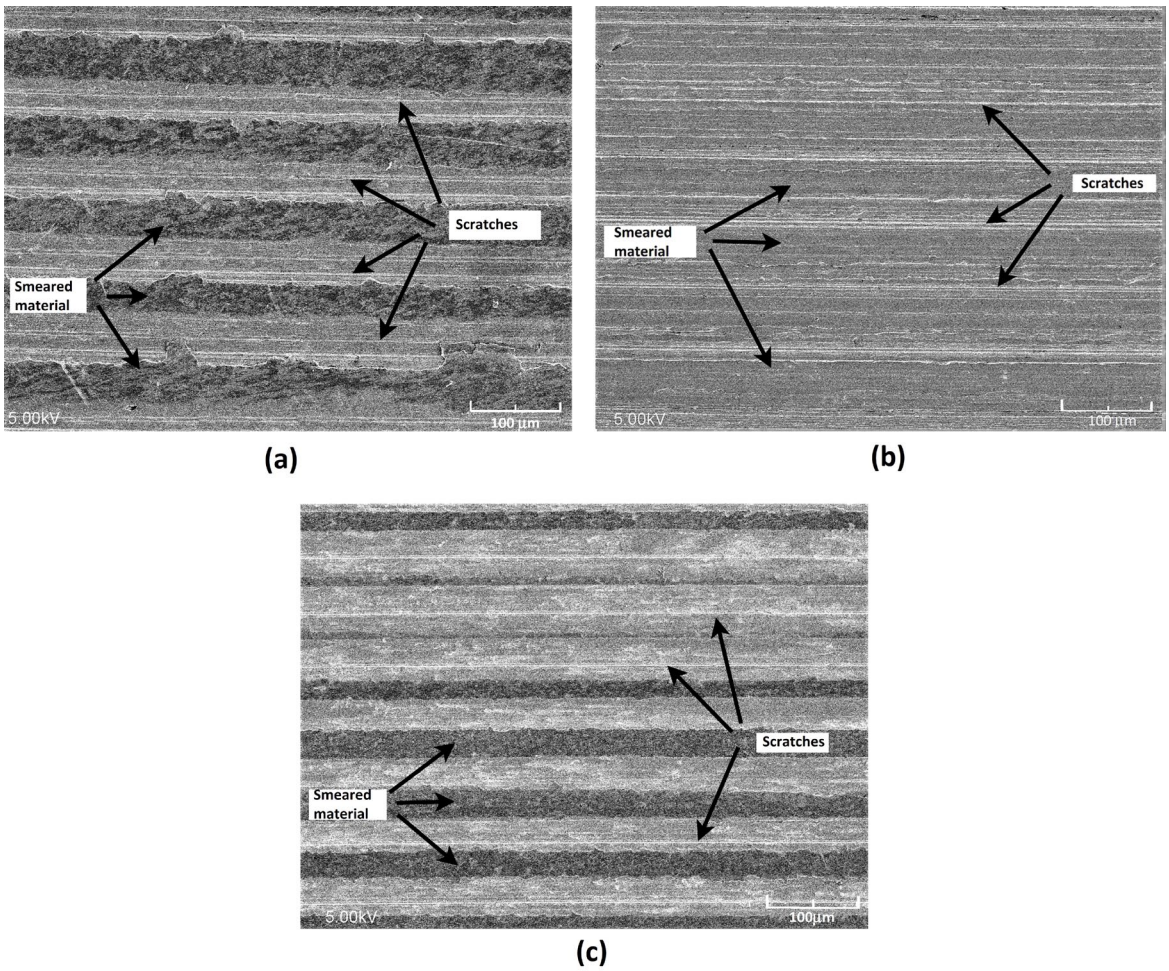

Fig. 12. Worn surfaces of SAE 660 bronze tested at (a) a pressure of 8 MPa (sliding velocity = 2 ms^{-1} and OFR = 1 $cm^3\ h^{-1}$) (b) a sliding velocity of 2.5 ms^{-1} (pressure = 6 MPa and OFR = 1 $cm^3\ h^{-1}$) (c) an OFR of 3 $cm^3\ h^{-1}$ (pressure = 6 MPa and sliding velocity = 2 ms^{-1}) for a SD of 20 km

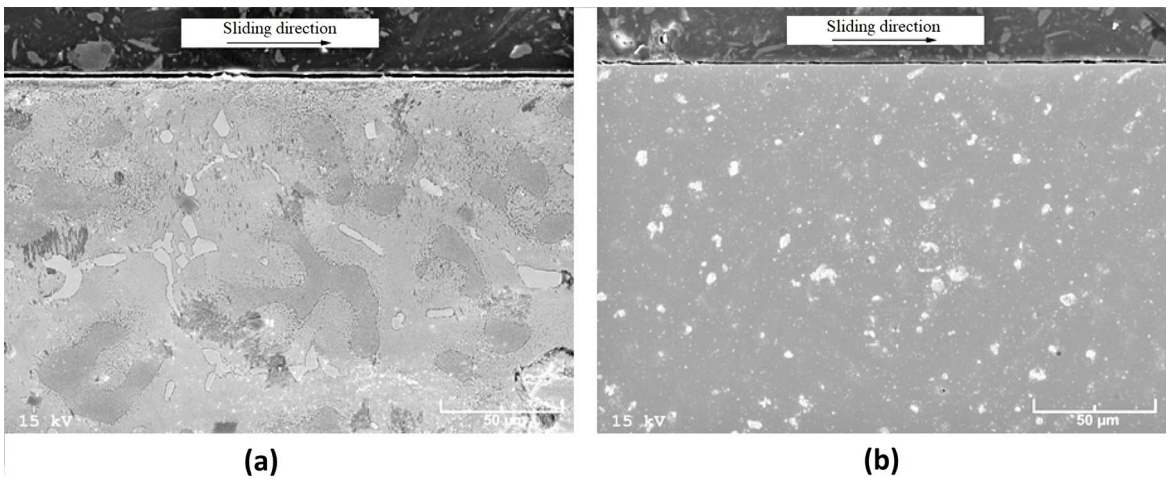

Fig. 13. Subsurface microstructures of the wear samples of (a) the zinc-based alloy and (b) SAE 660 bronze tested at a constant pressure (6 MPa), sliding velocity (2.5 ms^{-1}) and OFR (1 $cm^3\ h^{-1}$) for a SD of 108 km

from the disk surface due to centrifugal force, extends the time for the formation of oil film with sufficient thickness. This can cause an increment in the wear loss by extending the period of metal-to-metal contact between the sample and the disk surfaces.

Friction coefficient, temperature and wear loss of the materials tested at a constant pressure (6 MPa) and sliding velocity (2 ms^{-1}) decreased with increasing OFR, but the trend reversed above a level of 2.5 $cm^3\ h^{-1}$, Fig. 7(a)-(c). This observation can be explained according to the OFT. It is known that as the OFR increases the time or the number of revolutions necessary for the formation of oil film with adequate thickness decreases [23,24]. This also means that as the OFR increases the stage of

the boundary lubrication or duration of metal-to-metal contact decreases. Since most of the wear in the lubricated systems occurs during running-in period or boundary lubrication stage, the FC and wear loss are expected to decrease with increasing OFR.

The relationships between the operating conditions (pressure and sliding velocity) and the wear properties (wear loss, friction coefficient and temperature) of Zn-30Al-3Cu alloy are determined by nonlinear regression analysis at a constant OFR of 1 $cm^3\ h^{-1}$ for a SD of 20 km, and given below:

$$\Delta V = -0.0552 + 0.1681v - 0.0528p - 0.0163v^2 + 0.0138p^2 \quad (1)$$

$$FC = 0.0521 - 0.0028v - 0.0048p + 0.0062v^2 + 0.0002p^2 \quad (2)$$

$$T = 22.6949 - 2.8139v + 3.5563p + 2.7243v^2 - 0.0952p^2 \quad (3)$$

In these equations, ΔV is the wear loss [mm^3], FC is friction coefficient, T is temperature [°C], p is pressure [MPa] and v is sliding velocity [ms^{-1}]. The values of coefficient of determination (r^2) for these relationships were determined as 0.84, 0.87 and 0.95, respectively. This means that the values of ΔV, μ and T can be calculated in terms of p and v with the confidences of 84%, 87% and 95%, respectively.

Mathematical evaluation of these equations showed that the contact pressure is more effective on the wear loss and temperature of the zinc-based alloy, but pressure and sliding velocity have approximately the same influence on its friction coefficient, as seen in TABLE 3.

TABLE 3

Effect of test variables on the wear properties of the alloy

Test parameter	Percent change in test parameter (%)	Percent change in friction coefficient (%)	Percent change in temperature (%)	Percent change in wear loss (%)
Pressure	100	21.7	23.0	181.7
	200	27.3	34.0	453.1
Sliding velocity	100	20.7	7.9	93.9
	200	29.6	8.3	211.9

The FC, temperature and wear loss values of SAE 660 bronze tested at the same conditions were found to be much higher than those of the zinc-based alloy. This finding can be explained in terms of their microstructures, mechanical properties, and wear behavior. Zinc-based ternary or quaternary alloys are known to have an ideal microstructure for bearing purposes as consisting of soft and relatively hard phases. The soft phase facilitates sliding while the hard phase increases the load-carrying capacity [14,18,25]. In addition, zinc and aluminum oxide films form on the rubbing surfaces of the alloy samples also facilitate sliding and increase wear resistance [26]. Presence of smeared material and scratches on the wear samples of the bronze (Fig. 12) indicates that adhesion and abrasion are the major wear mechanisms for this material [16,18,27]. The scratches are probably made by the hard δ phase particles when they are removed from the sample surface due to wear. Since the abrasion becomes more evident with rising pressure and velocity, the values of the wear properties are expected to increase with these test variables.

SEM micrographs of the wear specimens of the experimental materials showed that the area of the smeared regions of the worn surfaces increased with increasing pressure and the sliding velocity, Figs 9-12. This can be associated with the observed increment in the wear loss with increasing pressure and the sliding velocity, Figs. 5(c) and 6(c). As the wear loss increases more wear material becomes available to adhere to the wear surfaces and this causes an increase in the smeared region. The EDS analysis showed that the smeared material is essentially oxidized zinc-based alloy. The oxygen content of this material was about 15%. The EDS analysis also showed that the zinc and aluminum contents of this material decreased considerably due to oxidation. The decreases were about 8% and 2% in zinc and aluminum contents, respectively. However, more scratches were noticed on the worn surface of the bronze samples compared to those of the alloy. These observations indicate that adhesive wear is the main mechanism for the alloy but wear of the bronze occurs due to both adhesion and abrasion [18,21].

No microstructural alterations were observed under the worn surface of the zinc-based alloy and the bronze even at a SD of 108 km, Fig. 13(a) and (b). This indicates that the levels of the pressure and sliding velocity were not sufficient to cause microstructural changes in the wear specimens of the experimental materials.

Finally, it can be concluded that the relationships between operating parameters and lubricated wear properties of zinc-aluminum based bearing alloys were determined for the first time in this work.

5. Conclusions

The following conclusions are drawn from the discussion of the experimental results of the present work:

1. Friction coefficient of both experimental materials decreases with increasing oil flow rate and contact pressure but shows a slight increase with sliding velocity.
2. Wear loss of the experimental materials increases with sliding distance, contact pressure and sliding velocity, but decreases slightly as the oil flow rate increases.
3. Under lubricated conditions wear loss, coefficient of friction and temperature of Zn-30Al-3Cu alloy can be calculated according to contact pressure and sliding velocity using the equations determined by nonlinear regression analysis and given in the Discussion section. These equations indicate that contact pressure is more influential on the wear loss and temperature of the alloy, but its friction coefficient has almost the same sensitivity to pressure and sliding velocity.

4. Zn-30Al-3Cu alloy shows lower friction coefficient, temperature, and wear loss than SAE 660 bronze during lubricated sliding.
5. Adhesion is the dominant wear mechanism for the zinc-based alloy, but the wear of the bronze occurs due to adhesion and abrasion under lubricated conditions.

Acknowledgment

The authors thank the technicians of the Mechanical Engineering Department of Karadeniz Technical University for their assistance.

REFERENCES

[1] E. Gebhardt, The Zn-corner of the Zn-Al-Cu ternary system, Z. Metallkd. **32**, 78-85 (1940).
[2] W. Köster, K. Moeller, The constitution and the volume changes of Zn-Cu-Al alloys. II. The relation of CuAl with the ternary phase, Z. Metallkd. **33**, 248-288 (1941).
[3] F.C. Porter, Zinc handbook: Properties, Processing and Use in Design (Mechanical Engineering), 1991 Marcel Dekker, New York.
[4] F.E. Goodwin, A.L. Ponikvar, Enineering Properties of Zinc Alloys, International Lead Zinc Research Organization, Third Edition, USA, 1989.
[5] E. Gervais, R.J. Barnhurst, C.A. Loong, An Analysis of Selected Properties of ZA Alloys, Jom.-J. Met. **37**, 43-47 (1985). DOI: https://doi.org/10.1007/BF03258743
[6] A.F. Skenazi, J. Pelerin, D. Coutsouradis, B. Magnus, M. Meeus, Some Recent Developments in the Improvement of the Mechanical Properties of Zinc Foundry Alloys, Metallwissenschaft und Technik **37**, 898-902 (1983).
[7] T.S. Calayag, The practicality of using zinc-aluminium alloys for friction-type bearings, 25th Annual Conference of Metallurgists, Toronto, Ontario, p. 305-313 (1986).
[8] K. Altorfer, Zinc Alloys Compete with Bronze in Bearings and Bushings, Met. Prog. **122**, 29-31 (1982).
[9] P. Delneuville, Tribological Behaviour of Zn-Al Alloys (ZA27) Compared with Bronze When Used as a Bearing Material with High Load and very Low Speed, Wear **105**, 283-292 (1985).
[10] W. Mihaichuk, Zinc-alloy bearing challenge the bronzes, Mach. Des. **53**, 133-137 (1981).
[11] Voest Alpine, Alzen 305, Alzen 501, White bronze 1976.
[12] B.K. Prasad, Effects of Silicon Addition and Test Parameters on Sliding Wear Characteristics of Zinc-Based Alloy Containing 37,5% Aluminium, Mater. T. JIM. **38**, 701-706 (1997). DOI: https://doi.org/10.2320/matertrans1989.38.701
[13] B.K. Prasad, Sliding Wear Response of a Zinc-based Alloy and its Composite and Comparison with a ray Cast Iron: Influence of External Lubrication and Microstructural Features, Mat. Sci. Eng. A-Struct. **392**, 427-439 (2005). DOI: https://doi.org/10.1016/j.msea.2004.10.031
[14] T. Savaşkan, Y. Alemdağ, Effects of Pressure and Sliding Speed on the Friction and Wear Properties of Al-40Zn-3Cu-2Si Alloy: A Comparative Study with SAE 65 Bronze, Mat. Sci. Eng. A-Struct. **496**, 517-523 (2008). DOI: https://doi.org/10.1016/j.msea.2008.06.008
[15] S. Murphy, T. Savaşkan, Comparative wear behavior of Zn-Al based alloys in an automotive engine application, Wear **98**, 151-161 (1984). DOI: https://doi.org/10.1016/0043-1648(84)90224-2
[16] Y. Alemdağ, T. Savaşkan, Mechanical and Tribological Properties of Al-40Zn-3Cu Alloys, Tribol. Int. **42**, 176-182 (2009). DOI: https://doi.org/10.1016/j.triboint.2008.04.008
[17] R.J. Barnhurst, Designing Zinc Alloy Bearings, J. Mater. Eng. **12**, 279-285 (1990).
[18] H.O. Tan, T. Savaşkan, Determination of Dry Wear Properties of Zn-30Al-Cu Bearing Alloys in Terms of Their Copper Content and Working Conditions Including Pressure and Sliding Velocity, J. Mater. Eng. Perform. **29**, 4794-4803 (2020). DOI: https://doi.org/10.1007/s11665-020-04976-7
[19] T. Savaşkan, A.P. Hekimoğlu, Microstructure and mechanical properties of Zn-15Al-based ternary and quaternary alloys, Mat. Sci. Eng. A-Struct. **603**, 52-57 (2014). DOI: https://doi.org/10.1016/j.msea.2014.02.047
[20] W. Krajewski, A.L. Greer, J. Buras, G. Piwowarski, P.K. Krajewski, New Developments of high-zinc Al-Zn-Cu-Mn cast alloys, Mater. Today-Proc. **10**, 306-311 (2019). DOI: https://doi.org/10.1016/j.matpr.2018.10.410
[21] T. Savaşkan, G. Pürçek, A.P. Hekimoğlu, Effect of Copper Content on the Mechanical and Tribological Properties of ZnAl27-based Alloys, Tribol. Lett. **15**, 257-263 (2003). DOI: https://doi.org/10.1023/A:1024817304351
[22] T. Savaşkan, O. Bican, Effects of Silicon Content on the Microstructural Features and Sliding Wear Properties of Zn-40Al-2Cu-(0-5)Si Alloys, Mat. Sci. Eng. A-Struct. **404**, 259-269 (2005). DOI: https://doi.org/10.1016/j.msea.2005.05.078
[23] I.M Hutchings, Tribology, Friction and Wear of Engineering Materials, 1992 Great Britain: Edward Arnold Publishers.
[24] J. Halling, Principles of Tribology, 1975 Oxford University Press, London.
[25] M. Babic, A. Vencl, S. Mitrovic, I. Bobic, Influence of T4 Heat Treatment on Tribological Behavior of Za27 Alloy Under Lubricated Sliding Condition, Tribol. Lett. **36**, 125-134 (2009). DOI: https://doi.org/10.1007/s11249-009-9467-x
[26] B.K. Prasad, Influence of Heat Treatment Parmeters on the Lubricated Sliding Wear Behavior of a Zinc Based Alloy, Wear **257**, 1137-1144 (2004). DOI: https://doi.org/10.1016/j.wear.2004.07.006
[27] O. Bican, T. Savaşkan, Influence of Test Conditions on the Lubricated Friction and Wear Behaviour of Al-25Zn-3Cu Alloy, Tribol. Lett. **37**, 175-182 (2010). DOI: https://doi.org/10.1007/s11249-009-9509-4